

## Spin-resolved and high-energy-resolution XPS studies of cobalt metal and a cobalt magnetic glass

L. E. Klebanoff,\* D. G. Van Campen, and R. J. Pouliot

*Department of Chemistry and Zettlemoyer Center for Surface Studies, Lehigh University, Bethlehem, Pennsylvania 18015*

(Received 23 August 1993)

The role of electron spin in photoelectric emission from the  $2s$ ,  $2p_{1/2}$ ,  $2p_{3/2}$ , and  $3p$  core levels of cobalt metal is investigated through a combination of spin-resolved x-ray-photoelectron spectroscopy (SRXPS) and high-energy-resolution XPS (HRXPS) studies. The sensitivity of the Co core-level spectra to a variation in the valence spin polarization is revealed by comparing the Co-metal data with SRXPS and HRXPS spectra from the amorphous cobalt-based ferromagnetic glass  $\text{Co}_{66}\text{Fe}_4\text{Ni}_1\text{B}_{14}\text{Si}_{15}$ . The results demonstrate explicitly the role of intra-atomic exchange in deep-core-level photoemission from Co, and reveal core-hole spin dependencies to core-hole-induced electron-hole-pair excitation, to the  $L_1L_{2,3}V$  Coster-Kronig transition rate, and to the rates of Auger transitions involving the valence band. The data also suggest that the reduction of the cobalt magnetic moment in the  $\text{Co}_{66}\text{Fe}_4\text{Ni}_1\text{B}_{14}\text{Si}_{15}$  glass results from the transfer of majority-spin  $3d$  electron density into the minority-spin  $3d$  band caused by a hybridization-induced weakening of the  $3d$  electron-electron interaction.

### I. INTRODUCTION

Core-level photoemission from  $3d$  transition-metal solids with a net spin in the valence shell has interested spectroscopists<sup>1-16</sup> and theorists<sup>15-22</sup> for many years. Several initial studies concerned the doublet structure observed in  $3s$  x-ray-photoelectron spectroscopy (XPS) spectra of Fe and Mn. The first interpretation of these structures<sup>1-5</sup> assigned them to "multiplet splitting." The intra-atomic exchange interaction is different for the two photoemission final-state configurations  $3s^13p^63d^n(2S+2L)$  and  $3s^13p^63d^n(2SL)$  for which the remaining  $3s$  spin is coupled, respectively, parallel and antiparallel to the initial-state  $3d$  spin  $S$ . The energy difference between these two final states is called the multiplet splitting.

The creation of a localized core hole at an atom in a metal is a significant electronic perturbation that can induce final-state electronic relaxations in the valence band of the  $N-1$  electron system.<sup>23</sup> For a metal with a fairly wide valence bandwidth (small electron-electron interaction), core-level ionization can excite delocalized low-energy electron-hole ( $e-h$ ) pairs in the valence band.<sup>24,25</sup> These intrinsic  $e-h$  pair excitations produce XPS line shapes that are asymmetric toward higher binding energy, as described theoretically by Doniach and Sunjic.<sup>26</sup> If the valence electron bandwidth is sufficiently narrow and the core-hole valence Coulomb interaction is strong enough, valence charge fluctuations can become localized at the core-hole site, leading to discrete satellite structure in both core and valence XPS spectra, as observed for Ni.<sup>27-29</sup>

In core-level XPS from metal ions in ionic compounds, it has been proposed that final-state charge transfer from the anionic ligand to the  $3d$  metal ion can alter the  $3d$  electron count.<sup>16</sup> Recent theoretical<sup>15,20,21</sup> and experimental<sup>10,12,15</sup> efforts have examined in considerable detail the circumstances for which these extra-atomic influences become important. The evolving view is that when the ligand-metal bond is highly ionic, charge transfer is not

likely and the  $3d$  electron count in the final state is the same as in the initial state.<sup>15</sup>

Multiplet splitting has been extensively investigated in the  $3s$  level of  $3d$  transition metals with spin-integrated XPS. However, spin-integrated studies have shed little light on the spin-dependent nature of photoemission from the deeper core levels because the exchange splittings and associated spectral variations could not be clearly resolved. We extend spin-resolved and high-energy-resolution photoemission studies to the deeper core levels in order to make contact with the large body of XPS data concerning the deep states, to provide line-shape data that characterizes the  $N-1$  electron response to core-hole spin, and to provide spectroscopic information for experimental methods that depend on the creation or existence of a deep core hole such as Auger-electron spectroscopy and x-ray-absorption and x-ray emission spectroscopies.

Cobalt is a fascinating metal of tremendous technological importance due in part to its ground-state ferromagnetism. Cobalt metal has a magnetic moment of  $1.72\mu_B$  per atom.<sup>30</sup> The ordered valence-band spin allows spin-resolved XPS (SRXPS) studies of core-valence intra-atomic exchange in deep-core-level photoemission. Cobalt lies immediately to the left of Ni in the Periodic Table, suggesting that its valence band is not as narrow as that of Ni, but also not as delocalized as the valence bands of metals with lower atomic number. Therefore, metallic cobalt might (or might not) display interesting spectroscopic complications due to valence electron correlation. The amorphous ferromagnetic metallic glass  $\text{Co}_{66}\text{Fe}_4\text{Ni}_1\text{B}_{14}\text{Si}_{15}$  belongs to a class of important technical ferromagnetic materials extensively used in transformer technology.<sup>31</sup> The Co atoms in the magnetic glass have a reduced magnetic moment of  $1.0\mu_B$  due to chemical bonding with the metalloid (B,Si) components. Thus a comparison of Co core-level SRXPS and high-energy-resolution XPS (HRXPS) spectra from the metal and the glass will reveal the role of a varying valence spin polarization on the spin dependence of deep-core-level photo-

emission. Section II gives the experimental details. A presentation and discussion of the SRXPS and HRXPS results are given in Sec. III. The relationship of these studies to previous experimental and theoretical work is described in Sec. IV. Conclusions are reviewed in Sec. V.

## II. EXPERIMENT

The HRXPS measurements employed Lehigh University's SCIENTA ESCA-300 x-ray-photoelectron spectrometer. This instrument combines a rotating Al anode with a monochromator to provide an intense source of monochromatic photons at 1486.6 eV. The energy analyzer is a large (300-mm mean radius) 180° hemispherical sector electrostatic energy analyzer with multichannel detection at the exit plane. The overall spectroscopic energy resolution was 0.32-eV full width at half maximum (FWHM) as judged from measurements of the width of the Fermi level of metallic Ni. The Co-metal sample for the HRXPS measurements was a 99.996% pure polycrystalline foil that was argon-ion sputtered at 1.5 kV for 80 min. The Co-glass sample  $\text{Co}_{66}\text{Fe}_4\text{Ni}_1\text{B}_{14}\text{Si}_{15}$  (Ref. 32) was a thin strip (0.003-in thick) that was argon-ion sputtered at 1.5 kV for 120 min to remove contaminants (mostly carbon and oxygen). Angle-dependent HRXPS studies revealed no evidence of surface segregation or preferential sputtering of the constituent elements of the magnetic glass. HRXPS analysis of the glass generally confirmed its composition.<sup>33</sup> The pressure in the analysis chamber during the HRXPS measurements was  $1.3 \times 10^{-9}$  Torr.

SRXPS measurements were performed with an instrument described in detail elsewhere.<sup>34</sup> Briefly, the instrument consists of a V.G. MkII 150° electrostatic energy analyzer coupled to a low-energy diffuse scattering electron spin detector.<sup>35</sup> The x-ray source was an unmonochromatized Mg  $K\alpha$  (1253.6 eV) x-ray tube operating at a power of 510 W. The overall energy resolution for the SRXPS measurements was 1.6-eV FWHM. The residual pressure in the SRXPS analysis chamber was  $2 \times 10^{-10}$  Torr during data acquisition.

For SRXPS studies, the cobalt-glass sample was formed into a loop with its free ends overlapped and clamped tightly together. The glass was magnetized by passing a dc current through coils wrapped around the legs of the loop. Magneto-optic Kerr effect (MOKE) measurements as well as measurements of the secondary electron polarization indicated that the Co glass could be very easily magnetized to saturation in the film plane.

The Co-metal sample for SRXPS study was a polycrystalline Co-metal film that was prepared by evaporating high-purity (99.996% pure) Co onto the cobalt-based magnetic glass. The strong ferromagnetic exchange coupling between Co metal and the magnetic glass produced a Co-metal film uniformly magnetized in the film plane (to be discussed) with negligible stray magnetic field. The thickness of the Co-metal films was not directly measured but was sufficient to *completely* suppress the B 1s (1063-eV kinetic energy) and the Si 2s (1104-eV kinetic energy) photoelectrons emanating from the underlying cobalt glass. This ensures that the Co-metal SRXPS spectra

reflect metallic Co and not Co in the magnetic glass, and also suggests that the Co-metal film thickness was in excess of  $\sim 60$  Å. A fresh Co film was prepared every 12–24 h as needed. The measured 30-eV spin polarization showed good stability throughout the measurements, and the summation of spin-resolved spectra was in excellent agreement with the corresponding spectra recorded with conventional XPS.

## III. RESULTS AND DISCUSSION

Spin-resolved core-level data for Co metal and the Co glass were collected into four channels  $N_L^+, N_L^-$  and  $N_R^+, N_R^-$ . Here,  $N_L^+$  represents the number of electrons diffusely scattered to the left ( $L$ ) from the Au target in the spin detector when the sample magnetization is positive (+).  $N_R^-$  is the number of electrons scattered to the right ( $R$ ) from the Au target when the sample magnetization has been reversed to the negative (–) direction. The electron beam polarization  $P$  can be expressed as<sup>36</sup>

$$P = \frac{N\uparrow - N\downarrow}{N\uparrow + N\downarrow} = \frac{1}{S} \left[ \frac{\sqrt{N_L^+ N_R^-} - \sqrt{N_L^- N_R^+}}{\sqrt{N_L^+ N_R^-} + \sqrt{N_L^- N_R^+}} \right], \quad (1)$$

where  $S$  is the analyzing power of the spin detector, known as the Sherman function.<sup>37</sup> SRXPS measurements using both (+) and (–) magnetizations removes from the polarization data apparatus asymmetry effects unrelated to the spin of the electron beam. The polarization data can be separated into individual  $N\uparrow$  and  $N\downarrow$  SRXPS spectra for the majority-spin ( $\uparrow$ -spin) and minority-spin ( $\downarrow$ -spin) photoelectrons, respectively, using the equations  $N\uparrow = 2N_{\text{tot}}(1+P)$ , and  $N\downarrow = 2N_{\text{tot}}(1-P)$ , where  $N_{\text{tot}} = (N_L^+ + N_L^- + N_R^+ + N_R^-)/4$ . The statistical error bars ( $\pm \delta N\uparrow\downarrow$ ) shown in the figures are calculated via the expression  $\delta N\uparrow\downarrow = N\uparrow\downarrow(1/S\sqrt{4N_{\text{tot}}})$ .<sup>36</sup> For all SRXPS measurements, the magnetizing current was switched from  $-0.5$  to  $0.5$  A (see Figs. 1 and 2) in order to flip and saturate the magnetization of the sample. The SRXPS count rates (summed over the  $L$  and  $R$  detectors, peak plus background) for the Co metal  $2p_{3/2}$ ,  $2p_{1/2}$ ,  $2s$ , and  $3p$  levels were approximately 3280, 2410, 1890, and 250  $\text{s}^{-1}$ , respectively.

Figures 1 and 2 display hysteresis curves for the Co glass and metallic Co acquired by measuring the spin polarization of 30-eV kinetic-energy secondary electrons as a function of the magnetic field applied to the Co glass. The glass hysteresis curve shows excellent agreement with hysteresis curves acquired with the MOKE technique (not shown), indicating that the near-surface magnetic properties of the glass (for example, the coercivity) are essentially identical to those of the bulk. This is consistent with the XPS data, that indicate no surface segregation of the glass components with argon-ion sputtering. When Co metal is evaporated onto the glass, the metal and glass couple strongly ferromagnetically. This strong coupling is indicated in Fig. 2 by the sharp magnetic reversal in the overlying metallic film when the magnetization of the underlying glass is flipped. The measured 30-eV polarization for the metal-Co overlayer is the same if

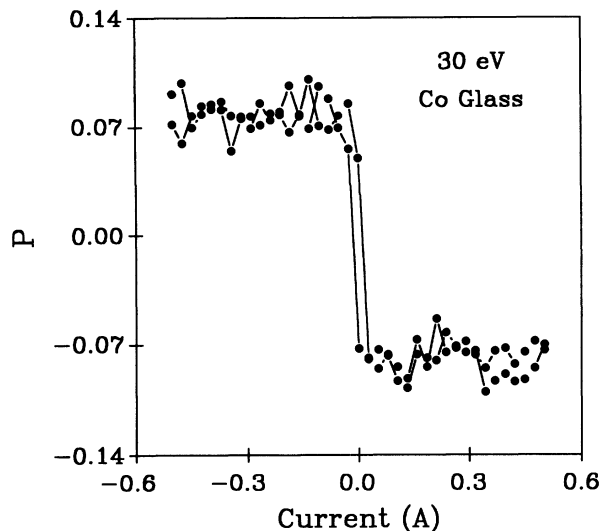


FIG. 1. A hysteresis curve for the magnetic glass  $\text{Co}_{66}\text{Fe}_4\text{Ni}_1\text{B}_{14}\text{Si}_{15}$  generated by measuring the spin polarization of 30-eV kinetic-energy secondary electrons vs the dc current applied to coils wrapped around the legs of the glass loop (see text).

the film thickness is reduced by two-thirds, or one-half. This finding, combined with the SRXPS data to be presented, indicate a Co film with a saturated magnetization in the film plane. The 30-eV polarization of the Co film is  $0.115 \pm 0.01$ . The theoretical valence-band spin polarization for Co metal is 0.173. Thus, in contrast to Fe and Ni metallic glasses,<sup>38</sup> it seems that for Co the theoretical valence-band spin polarization does not quantitatively predict the observed 30-eV spin polarization. The spin polarization of the Co 13-eV kinetic-energy secondary electrons ( $0.15 \pm 0.01$ ) was in good agreement

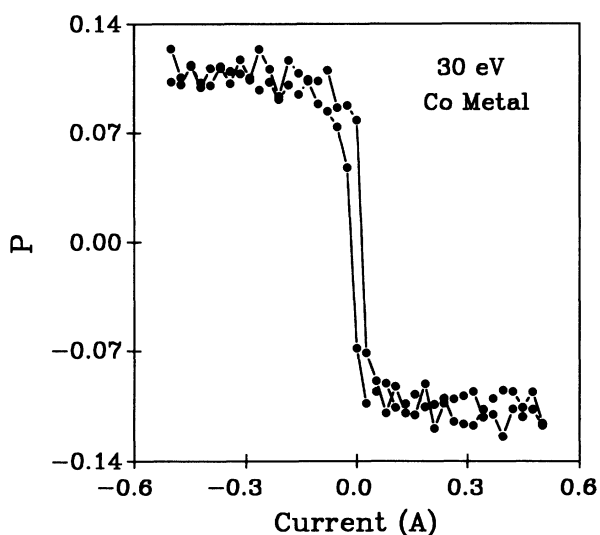


FIG. 2. A hysteresis curve for Co metal evaporated onto the Co glass substrate. The plot was generated by measuring the spin polarization of 30-eV kinetic-energy secondary electrons vs the dc current applied to coils wrapped around the legs of the magnetic glass substrate (see text).

with previous results from Co metal.<sup>39</sup>

The magnetic moment per cobalt atom for the alloy  $\text{Co}_{66}\text{Fe}_4\text{Ni}_1\text{B}_{14}\text{Si}_{15}$  has not been reported. However, for the closely related alloy  $\text{Co}_{75}\text{Si}_{15}\text{B}_{10}$  the Co atoms have a reduced magnetic moment of  $1.0\mu_B$ .<sup>40</sup> For the alloy  $\text{Co}_{71}\text{B}_{29}$ , the magnetic moment per cobalt atom is reported to be  $0.98\mu_B$ .<sup>41</sup> These two measurements demonstrate that B and Si have very similar effects on the Co atomic magnetic moment, and that amorphous alloys with similar cobalt/metalloid stoichiometric ratios have similar values for the cobalt magnetic moment. Since the alloys  $\text{Co}_{66}\text{Fe}_4\text{Ni}_1\text{B}_{14}\text{Si}_{15}$  and  $\text{Co}_{71}\text{B}_{29}$  have similar cobalt/metalloid stoichiometric ratios, and B and Si behave similarly, it is highly likely that the magnetic moment per cobalt atom in the  $\text{Co}_{66}\text{Fe}_4\text{Ni}_1\text{B}_{14}\text{Si}_{15}$  glass is  $\sim 1.0\mu_B$ .

If all of the Co atoms in the glass retain a  $1.72\mu_B$  magnetic moment, the theoretical spin polarization of the glass would be 0.152 or 12.1% smaller than the metal. If all of the Co atoms in the glass possess a magnetic moment of  $1.0\mu_B$ , as estimated above, then the theoretical glass spin polarization would be 0.093 or 46% smaller than the metal. The observed 30-eV polarization for the glass is  $0.085 \pm 0.01$ , or 26% smaller than that of the metal. Thus the 30-eV polarization data for the glass indicates Co atoms with a reduced spin polarization, but are not quantitatively consistent with a value of  $1.0\mu_B$  for the magnetic moment on the Co atoms in the glass.

Figure 3 displays a comparison of HRXPS spectra for the valence bands of Co metal and Co-based glass. The glass spectrum largely reflects the Co 3d level due to its dominant photoelectric cross section and the large concentration of Co in the glass. The FWHM of the glass

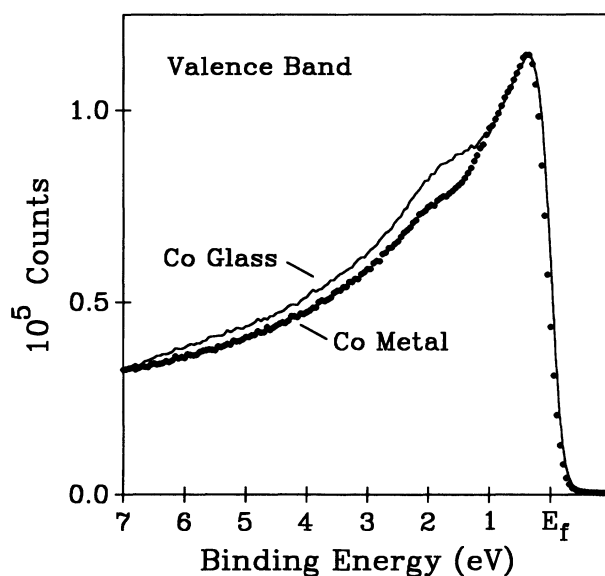


FIG. 3. A comparison of HRXPS spectra of the valence-band region for Co metal (dots) and  $\text{Co}_{66}\text{Fe}_4\text{Ni}_1\text{B}_{14}\text{Si}_{15}$  (line). The energy resolution for both measurements was 0.32-eV FWHM. The spectra have been normalized at the valence-band maximum. The valence-band FWHM value for Co metal is 3.32 eV; the valence-band FWHM for  $\text{Co}_{66}\text{Fe}_4\text{Ni}_1\text{B}_{14}\text{Si}_{15}$  is 3.72 eV.

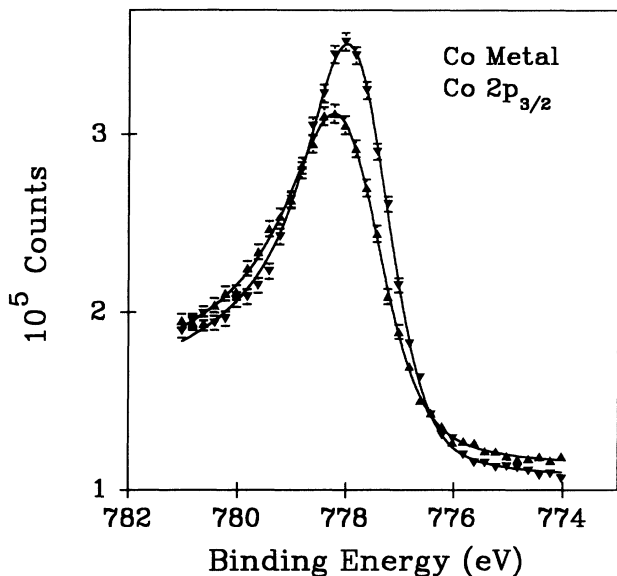


FIG. 4. Separate  $N\uparrow$  and  $N\downarrow$  SRXPS spectra for Co  $2p_{3/2}$  majority-spin ( $\blacktriangle$ ) and minority-spin ( $\blacktriangledown$ ) photoelectrons of Co metal. The lines through the data are the result of a simplex fit to each spin component using a single Doniach-Sunjic line shape convoluted with a Gaussian of 1.6-eV FWHM.

valence band is 0.40 eV larger than that of the metal. This finding is consistent with a broadening of the Co  $3d$  valence band by hybridization with the B and Si valence orbitals. This hybridization (and not charge transfer from the metalloid atoms to the metal atom) is thought to reduce the  $3d$  magnetic moment on Co in the glass by weakening the  $3d$  electron-electron interaction.<sup>42</sup> We shall see that the SRXPS and HRXPS data are in fact qualitatively consistent with a sizable *reduction* of the local magnetic moment on the cobalt atoms in the amorphous glass. Thus the broadening observed in Fig. 3 cannot be attributed to an enhanced  $3d$  exchange splitting for the glass.

#### Co $2p_{3/2}$ results

The Co  $2p_{3/2}$  level gives the most intense core-level peak in the XPS spectrum. Unfortunately, using a photon energy of 1486.6 eV, the Co  $L_3M_{2,3}V$  Auger peak interferes with the Co  $2p_{3/2}$  peak, making high-resolution

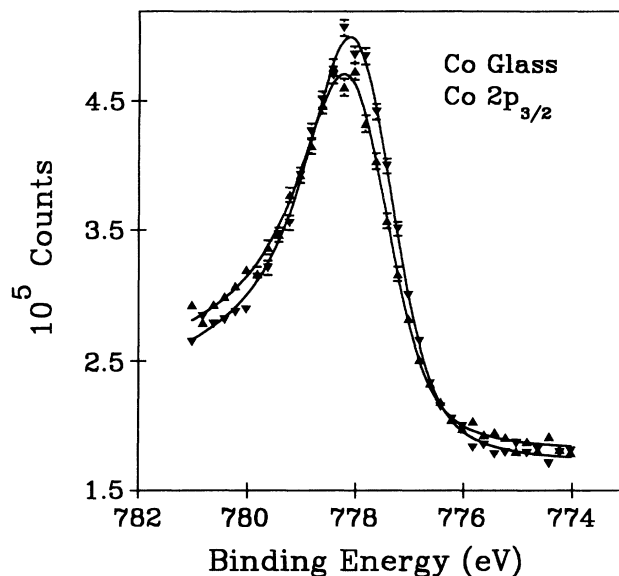


FIG. 5. Separate  $N\uparrow$  and  $N\downarrow$  SRXPS spectra for Co  $2p_{3/2}$  majority-spin ( $\blacktriangle$ ) and minority-spin ( $\blacktriangledown$ ) photoelectrons of  $\text{Co}_{66}\text{Fe}_4\text{Ni}_1\text{B}_{14}\text{Si}_{15}$ . The lines through the data are the result of a simplex fit to each spin component using a single Doniach-Sunjic line shape convoluted with a Gaussian of 1.6-eV FWHM.

study of the Co  $2p_{3/2}$  level impossible. Fortunately, this is not a problem for the SRXPS studies that employ a photon energy of 1253.6 eV.

Figures 4 and 5 display SRXPS spectra for the Co  $2p_{3/2}$  level for metallic Co and Co glass, respectively. For the  $2p_{3/2}$  level, we have fit a single Doniach-Sunjic (DS) line, convoluted with a 1.6-eV Gaussian, to the  $N\uparrow$  (majority-spin) and  $N\downarrow$  (minority-spin) components over the limited binding-energy range 781–774 eV. Results for the DS fits to all of the SRXPS spectra can be found in Table I. The  $2p_{3/2}$  fit is limited in energy because the low intensity Mg  $K\alpha_{3,4}$  x-ray satellites extending up to 10 eV from the Co  $2p_{1/2}$  peak at  $\sim 793$  eV interfere slightly with the spectral intensity from the  $2p_{3/2}$  level past 782-eV binding energy. The single-component DS fits are quite satisfactory, and for the metal yield the following spin-dependent values for the spectral binding energy ( $E_B\uparrow, \downarrow$ ), the singularity index ( $\alpha\uparrow, \downarrow$ ) that accounts for the  $e$ - $h$  pair-induced asymmetry of the XPS line, and the FWHM Lorentzian broadening ( $\Gamma\uparrow, \downarrow$ ):  $N\uparrow$ ,  $E_B\uparrow$

TABLE I. A compilation of the SRXPS results for Co metal and  $\text{Co}_{66}\text{Fe}_4\text{Ni}_1\text{B}_{14}\text{Si}_{15}$ .

|            | $E_B\uparrow - E_B\downarrow$ (eV) | $\alpha\uparrow$ | $\alpha\downarrow$ | $\Gamma\uparrow$ (eV) | $\Gamma\downarrow$ (eV) | $I\uparrow/I\downarrow$ |
|------------|------------------------------------|------------------|--------------------|-----------------------|-------------------------|-------------------------|
| Co metal   |                                    |                  |                    |                       |                         |                         |
| $2p_{3/2}$ | $0.18\pm 0.05$                     | $0.39\pm 0.02$   | $0.36\pm 0.02$     | $0.73\pm 0.1$         | $0.49\pm 0.1$           | $0.87\pm 0.03$          |
| $2p_{1/2}$ | $0.07\pm 0.05$                     | $0.41\pm 0.02$   | $0.30\pm 0.02$     | $1.24\pm 0.1$         | $1.42\pm 0.1$           | $1.31\pm 0.03$          |
| $2s$       | $0.65\pm 0.3$                      | $0.44\pm 0.04$   | $0.50\pm 0.04$     | $11.4\pm 0.5$         | $6.3\pm 0.5$            | $1.2\pm 0.1$            |
| $3p$       | $0.10\pm 0.05$                     | $0.46\pm 0.02$   | $0.38\pm 0.02$     | $1.3\pm 0.1$          | $1.4\pm 0.1$            | $0.81\pm 0.04$          |
| Co glass   |                                    |                  |                    |                       |                         |                         |
| $2p_{3/2}$ | $0.06\pm 0.05$                     | $0.35\pm 0.02$   | $0.31\pm 0.02$     | $0.65\pm 0.1$         | $0.64\pm 0.1$           | $0.92\pm 0.03$          |
| $2p_{1/2}$ | $0.11\pm 0.05$                     | $0.41\pm 0.02$   | $0.37\pm 0.02$     | $1.16\pm 0.1$         | $0.99\pm 0.1$           | $1.20\pm 0.03$          |
| $2s$       | $0.49\pm 0.3$                      | $0.45\pm 0.04$   | $0.41\pm 0.04$     | $8.1\pm 0.5$          | $8.6\pm 0.5$            | $1.0\pm 0.1$            |
| $3p$       | $0.03\pm 0.05$                     | $0.41\pm 0.02$   | $0.36\pm 0.02$     | $1.4\pm 0.1$          | $1.6\pm 0.1$            | $0.90\pm 0.03$          |

$=777.84 \pm 0.030$  eV,  $\alpha \uparrow = 0.39 \pm 0.020$ , and  $\Gamma \uparrow = 0.73 \pm 0.10$  eV. For the  $N \downarrow$  component we derive the spectral values  $E_B \downarrow = 777.66 \pm 0.030$  eV,  $\alpha \downarrow = 0.36 \pm 0.02$ , and  $\Gamma \downarrow = 0.49 \pm 0.10$  eV. The SRXPS data reveal a Co-metal  $2p_{3/2}$  spin-dependent (exchange) splitting of  $0.18 \pm 0.05$  eV. The spin-dependent  $2p_{3/2}$  intensity ratio is  $I \uparrow / I \downarrow = 0.87 \pm 0.03$ . Errors quoted on spectral parameters are derived from statistical considerations, as well as by repetitious SRXPS measurements. It should be noted that SRXPS measurements of the  $2p_{3/2}$  and  $2p_{1/2}$  levels of nonmagnetic copper show no spin-dependent splitting, no spin dependence to  $\alpha$  or  $\Gamma$ , and  $I \uparrow / I \downarrow = 1.0$  to within the experimental errors quoted for the Co  $2p_{3/2}$  and  $2p_{1/2}$  SRXPS measurements.

It is interesting that the core-valence exchange coupling is sizable for the  $2p_{3/2}$  level even though the  $2p$ - $3d$  exchange interaction is spatially limited by the  $\sim 0.13$ -Å radial extent of the  $2p_{3/2}$  orbital.<sup>43</sup> One expects the  $N \downarrow$  component to have a smaller binding energy than the  $N \uparrow$  component, since the emission of a  $\downarrow$ -spin electron leaves the remaining ion in a high-spin final state that is energetically favored by intra-atomic exchange.

The Lorentzian width  $\Gamma \uparrow$  of the  $2p_{3/2}$   $N \uparrow$  component is larger than the width  $\Gamma \downarrow$  of the  $N \downarrow$  component. Thus the lifetime of an  $\uparrow$ -spin  $2p_{3/2}$  hole is shorter than that for a  $\downarrow$ -spin  $2p_{3/2}$  hole. The  $2p_{3/2}$  ( $L_3$ ) lifetime is determined by the rates of three Auger transitions  $L_3VV$ ,  $L_3M_{2,3}V$ , and  $L_3M_{2,3}M_{2,3}$ , whose approximate relative cross sections are 1.0, 0.75, and 0.5, respectively. Spin is theoretically conserved in the nonrelativistic Auger filling of a core hole due to the spin-independent Coulomb interaction governing the Auger decay.<sup>44,45</sup> The  $L_3VV$  transition rate should be larger for an  $\uparrow$ -spin  $L_3$  hole since an excess of  $\uparrow$ -spin electrons exists for both of the upper levels ( $V, V$ ) involved in the Auger decay. By similar reasoning, the  $L_3M_{2,3}V$  transition rate should, to a lesser extent, also show a dependence on the  $L_3$  core-hole spin. The  $L_3M_{2,3}M_{2,3}$  transition rate would not be expected to show a dependence on the spin of the  $L_3$  hole, since there is no spin imbalance in the levels involved in the Auger decay.

The  $2p_{3/2}$  SRXPS spectra for the Co-based glass are shown in Fig. 5. The DS fit results can be summarized as follows:  $N \uparrow$ ,  $E_B \uparrow = 777.88 \pm 0.03$  eV,  $\alpha \uparrow = 0.35 \pm 0.02$ , and  $\Gamma \uparrow = 0.65 \pm 0.1$  eV. For  $N \downarrow$ ,  $E_B \downarrow = 777.82 \pm 0.03$  eV,  $\alpha \downarrow = 0.31 \pm 0.02$ , and  $\Gamma \downarrow = 0.64 \pm 0.1$  eV. The reduced exchange splitting for the glass  $2p_{3/2}$  level is  $0.060 \pm 0.05$  eV, compared with that of the metal,  $0.18 \pm 0.05$  eV, and clearly demonstrates that as the valence electron-spin polarization decreases, the spin-dependent  $2p_{3/2}$  splitting decreases. The  $2p_{3/2}$   $I \uparrow / I \downarrow$  ratio is  $0.92 \pm 0.03$ . All reported ratios are based on integrated intensities from the DS fits.

As the  $3d$  magnetic moment decreases, the spin dependence of the  $2p_{3/2}$  core-hole lifetime  $\Gamma$  diminishes, with the spin-resolved values  $\Gamma \uparrow$  and  $\Gamma \downarrow$  for the glass converging toward the average of  $\Gamma \uparrow$  and  $\Gamma \downarrow$  for the metal. Since the absolute spin-resolved core filling rates are determined by the  $\uparrow$ -spin and  $\downarrow$ -spin populations in the  $3d$  valence band, the convergence of  $\Gamma \uparrow$  and  $\Gamma \downarrow$  indicates

that there exists (per Co atom) fewer  $\uparrow$ -spin  $3d$  electrons and more  $\downarrow$ -spin  $3d$  electrons in the glass than found in the metal. This is, of course, consistent with a lower magnetic moment for the Co atoms in the glass, but also suggests that the reduction of the magnetic moment is achieved by the transfer of  $\uparrow$ -spin  $3d$  valence electron density into the  $\downarrow$ -spin  $3d$  valence band, thereby producing fewer  $\uparrow$ -spin electrons and more  $\downarrow$ -spin electrons per Co atom. This would be a direct confirmation that Co  $3d$  hybridization with the metalloid valence orbitals weakens the  $3d$  electron-electron interaction in the glass,<sup>42</sup> thereby causing spin pairing in the valence band. The data are *inconsistent* with a reduced moment caused by the transfer of charge into the unoccupied minority-spin band from the metalloid components,<sup>46</sup> since this mechanism would not vary the  $\uparrow$ -spin population, and therefore not affect the  $\Gamma \uparrow$  value.

When an intrinsically asymmetric XPS line shape is convoluted with symmetric instrumental (Gaussian) and lifetime (Lorentzian) broadenings, the apparent peak maximum is shifted toward higher binding energy from the true peak position that would be observed in the absence of an asymmetry. According to the theory of Doniach and Sunjic,<sup>26</sup> for a given  $\alpha$  and  $\Gamma$  the peak maximum differs from the true peak position by  $(\Gamma/2)\cot[\pi/(2-\alpha)]$ . Thus an estimate of peak splitting based solely on the positions of peak maxima would overestimate the true energy splitting. The fact that  $\Gamma$  and  $\alpha$  are themselves spin dependent places a great importance on the need to fit the data to physically reasonable line shapes, rather than relying on a visual estimate of peak separation, in order to determine exchange splittings.

The XPS line-shape asymmetry is intrinsic to the photoelectron spectrum. The asymmetric component exists at the moment of photoelectric excitation, and is *not* produced with significant intensity (over the energy range of the fits) by extrinsic inelastic scattering of the outgoing photoelectrons.<sup>47,48</sup> Therefore, an analysis of these SRXPS data must incorporate the asymmetry of the line shape without an added inelastic background, as done in this work. Any analysis incorporating a background subtraction that reduces the spectral intensity on the high-binding-energy side of the peak to zero cannot extract accurate line-shape information. This point has been made eloquently by Citrin, Wertheim, and Baer.<sup>47</sup>

#### Co $2p_{1/2}$ results

Figure 6 compares HRXPS spectra of the Co  $2p_{1/2}$  level for metallic Co and the Co-based glass. The spectra are normalized to each other at the peak maxima. It is clear from Fig. 6 that the Co metal  $2p_{1/2}$  spectrum is somewhat broader than the Co-glass spectrum. The SRXPS spectra for the metal and the glass are shown in Figs. 7 and 8, respectively.

The  $N \uparrow$  and  $N \downarrow$  Co  $2p_{1/2}$  metal spectra of Fig. 7 are both fit well with a single DS line convoluted with a Gaussian of 1.6-eV FWHM. For  $N \uparrow$  we find  $E_B = 792.80 \pm 0.03$  eV, with  $\alpha \uparrow = 0.41 \pm 0.02$  and  $\Gamma \uparrow = 1.24 \pm 0.1$  eV. For  $N \downarrow$  we find  $E_B \downarrow = 792.73 \pm 0.03$

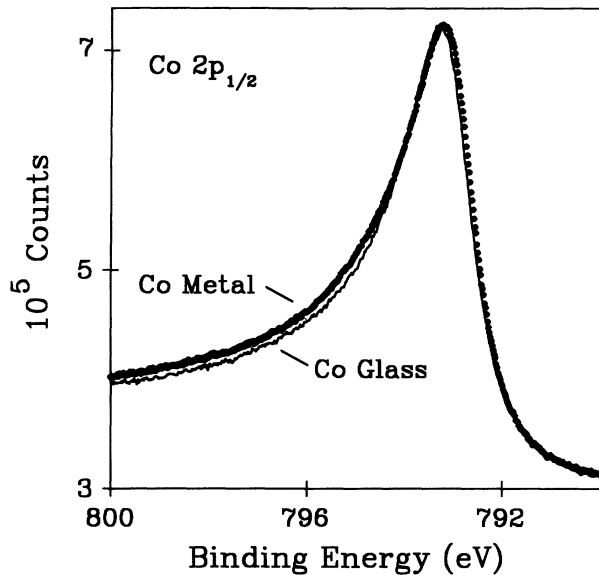


FIG. 6. HRXPS spectra for the Co  $2p_{1/2}$  level of Co metal (dots) and  $\text{Co}_{66}\text{Fe}_4\text{Ni}_1\text{B}_{14}\text{Si}_{15}$  (line). The spectra have been normalized at the peak maxima.

eV, with  $\alpha\downarrow=0.30\pm0.02$  and  $\Gamma\downarrow=1.42\pm0.1$  eV. Thus a small  $2p_{1/2}$  "exchange splitting" of  $0.07\pm0.05$  eV is observed. The  $I\uparrow/I\downarrow$  value is  $1.31\pm0.03$ . The  $N\uparrow$  and  $N\downarrow$   $2p_{1/2}$  spectra differ significantly in their singularity index. Evidently, for the  $2p_{1/2}$  level, the  $\uparrow$ -spin core hole couples more strongly to the valence shell  $e-h$  pair excitation spectrum, leading to a significantly more asymmetric  $2p_{1/2}$  line shape.

The solid lines shown in Fig. 8 for the Co-glass  $2p_{1/2}$  level are also fits to each spin component using single DS line shapes. The results for the  $N\uparrow$  component are

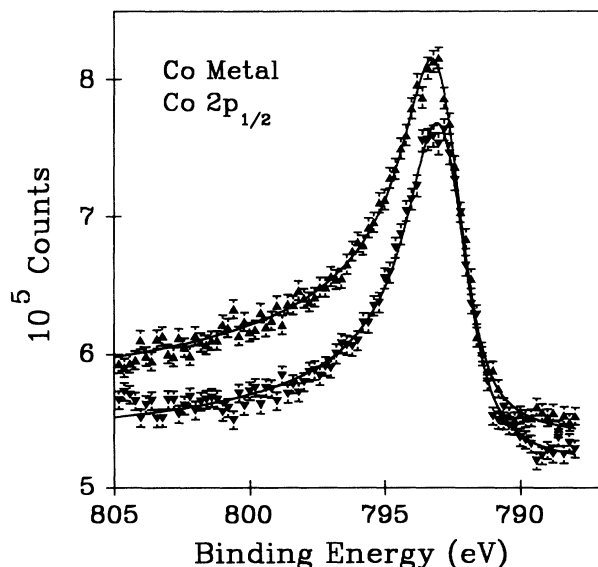


FIG. 7. Separate  $N\uparrow$  and  $N\downarrow$  SRXPS spectra for Co  $2p_{1/2}$  majority-spin ( $\blacktriangle$ ) and minority-spin ( $\blacktriangledown$ ) photoelectrons of Co metal. The lines through the data are the result of a simplex fit to each spin component using a single Doniach-Sunjić line shape convoluted with a Gaussian of 1.6-eV FWHM.

$E_B\uparrow=792.77\pm0.03$  eV,  $\alpha\uparrow=0.41\pm0.02$ , and  $\Gamma\uparrow=1.16\pm0.1$  eV. The results for the  $N\downarrow$  component are  $E_B\downarrow=792.66\pm0.03$  eV,  $\alpha\downarrow=0.37\pm0.02$ , and  $\Gamma\downarrow=0.99\pm0.1$  eV. Thus a spin-dependent  $2p_{1/2}$  splitting of  $0.11\pm0.05$  eV is observed for the cobalt magnetic glass. Interestingly, the metallic and glass  $2p_{1/2}$  splittings are very similar. The  $2p_{1/2}$   $\Gamma\uparrow$  and  $\Gamma\downarrow$  values show a complicated variation from metal to glass. The spin-dependent intensity ratio is  $I\uparrow/I\downarrow=1.20\pm0.03$ .

The differences between the  $2p_{1/2}$   $\alpha\uparrow$  and  $\alpha\downarrow$  values for the metal ( $0.11\pm0.03$ ) is larger than the corresponding difference for the glass ( $0.04\pm0.03$ ). This demonstrates that as the spin polarization of the valence band decreases, the spin dependence of the singularity index decreases. This finding was not obvious from the  $2p_{3/2}$  SRXPS data, perhaps due to the smaller  $2p_{3/2}$   $\alpha\uparrow-\alpha\downarrow$  difference observed for the metal.

An important result for the  $2p_{1/2}$  level is that the  $N\uparrow$  component has a higher binding energy than the  $N\downarrow$  component. This result is generally consistent with expectations based on multiplet splitting of high-spin and low-spin XPS final states. One could attempt to model the spin splitting of the  $2p_{1/2}$  level as a Zeeman-like splitting due to a magnetic field arising from the valence magnetization. Such a mechanism has been put forth to explain magnetic circular dichroism measurements.<sup>49</sup> However, a Zeeman-like model would predict that the  $2p_{1/2}$   $N\uparrow$  component would have a lower binding energy than the  $2p_{1/2}$   $N\downarrow$  component, in disagreement with the SRXPS observations.

It is apparent from Figs. 6–8 that there is no evidence for a "correlation satellite" peak located 4.5 eV to higher binding energy in the Co  $2p_{1/2}$  core-level spectra. Previous work<sup>50</sup> has claimed the existence of such a feature in analogy with the 6-eV satellite observed in XPS spectra

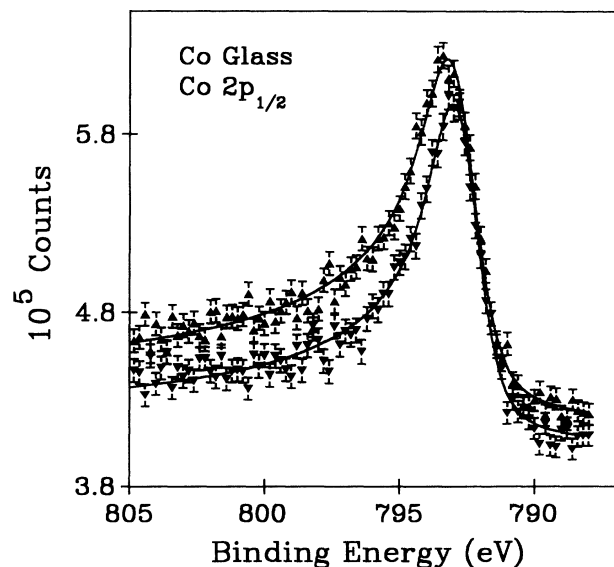


FIG. 8. Separate  $N\uparrow$  and  $N\downarrow$  SRXPS spectra for Co  $2p_{1/2}$  majority-spin ( $\blacktriangle$ ) and minority-spin ( $\blacktriangledown$ ) photoelectrons of  $\text{Co}_{66}\text{Fe}_4\text{Ni}_1\text{B}_{14}\text{Si}_{15}$ . The lines through the data are the result of a simplex fit to each spin component using a single Doniach-Sunjić line shape convoluted with a Gaussian of 1.6-eV FWHM.

of Ni core levels. Both the HRXPS and SRXPS measurements show conclusively that such a satellite does not exist, indicating that the valence band of metallic Co is not sufficiently narrow to support localized  $3d$  charge fluctuations that would produce discrete satellite structure in XPS.

#### Co 2s results

Figure 9 compares HRXPS  $2s$  XPS spectra for metallic Co and the Co-based metallic glass. For this comparison, the spectra have been normalized at the peak maxima. The Co-metal  $2s$  spectrum is significantly wider than that of the glass. Other than this, there is no clear evidence for multiplet structure in these Co  $2s$  HRXPS spectra.

The Co  $2s$  SRXPS data of Figs. 10 and 11 reveal that these line shapes are in fact strongly dependent on the electron spin, indicating that  $2s$ - $3d$  exchange is sizable and observable. SRXPS studies of the Co  $2s$  level are challenging because the  $2s$  level is quite broad and resides on a large spectral background. These characteristics make it difficult to acquire  $2s$  SRXPS spectra with a satisfactory statistical quality. The  $2s$   $N\uparrow$  and  $N\downarrow$  spectra for Co metal in Fig. 9 are each fit to a single DS component over the limited binding-energy range 905–934 eV.<sup>51</sup> The results of the fits are as follows:  $N\uparrow$ ,  $E_B\uparrow = 923.50 \pm 0.2$ ,  $\alpha\uparrow = 0.44 \pm 0.04$ , and  $\Gamma\uparrow = 11.4 \pm 0.5$  eV;  $N\downarrow$ ,  $E_B\downarrow = 922.85 \pm 0.2$  eV, with  $\alpha\downarrow = 0.50 \pm 0.04$  and  $\Gamma\downarrow = 6.3 \pm 0.5$  eV. Thus a  $2s$  “exchange splitting” of  $0.65 \pm 0.3$  eV is observed. The Co  $2s$  metal  $I\uparrow/I\downarrow$  ratio is  $1.2 \pm 0.1$ . The  $N\uparrow$  component has a much larger lifetime broadening than the  $N\downarrow$  component. The lifetime of the  $2s$  level is thought to be determined by the rate of  $L_1L_{2,3}X$  Coster-Kronig transitions, of which the  $L_1L_{2,3}V$  transition dominates.<sup>52</sup> The strong spin dependence of the  $2s$  width indicates that the  $L_1L_{2,3}V$  transitions con-

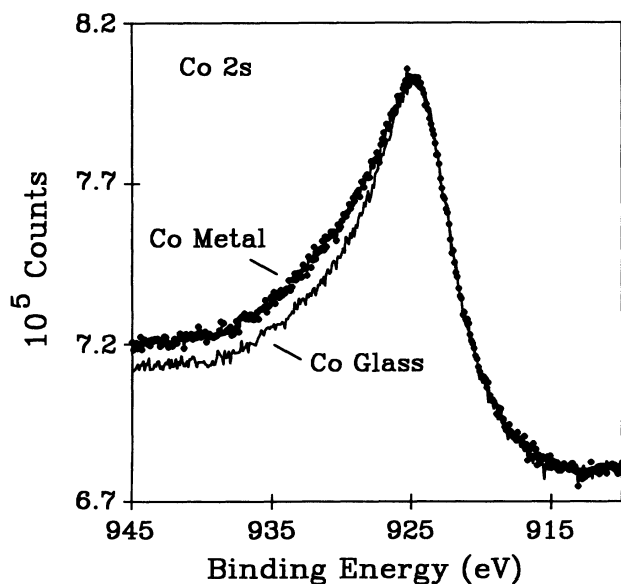


FIG. 9. HRXPS spectra for the Co  $2s$  level of Co metal (dots) and  $\text{Co}_{66}\text{Fe}_4\text{Ni}_1\text{B}_{14}\text{Si}_{15}$  (line). The spectra have been normalized at the peak maxima.

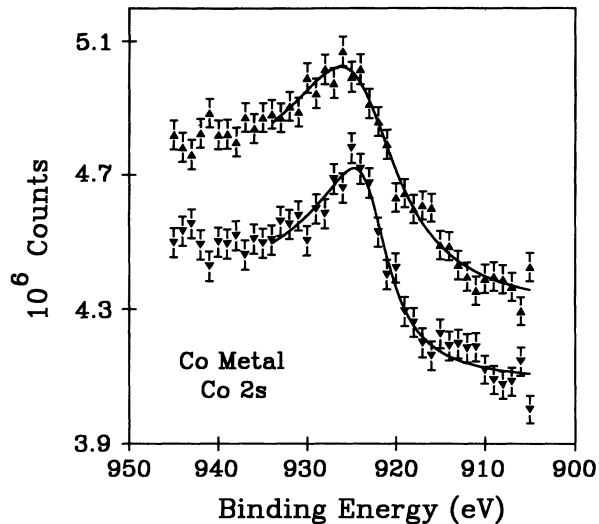


FIG. 10. Separate  $N\uparrow$  and  $N\downarrow$  SRXPS spectra for Co  $2s$  majority-spin ( $\blacktriangle$ ) and minority-spin ( $\blacktriangledown$ ) photoelectrons of Co metal. The lines through the data are the result of a simplex fit to each spin component using a single Doniach-Sunjić line shape convoluted with a Gaussian of 1.6-eV FWHM. The binding-energy range for the fit was 934–905 eV.

serve spin, and that the predominance of  $\uparrow$ -spin electrons in the valence band leads to a larger Coster-Kronig transition rate for the filling of  $\uparrow$ -spin  $2s$  holes in Co.

The Co  $2s$  spectrum for the magnetic glass is shown in Fig. 11. Fitting with a single DS line shape over the range 905–934 eV, one obtains  $E_B\uparrow = 923.38 \pm 0.2$  eV, with  $\alpha\uparrow = 0.45 \pm 0.04$  and  $\Gamma\uparrow = 8.1 \pm 0.5$  eV, for the  $N\uparrow$  component. For the  $N\downarrow$  component, we obtain  $E_B\downarrow = 922.89 \pm 0.2$  eV, with  $\alpha\downarrow = 0.41 \pm 0.04$  and  $\Gamma\downarrow = 8.6 \pm 0.5$  eV. The Co  $2s$  glass intensity ratio is

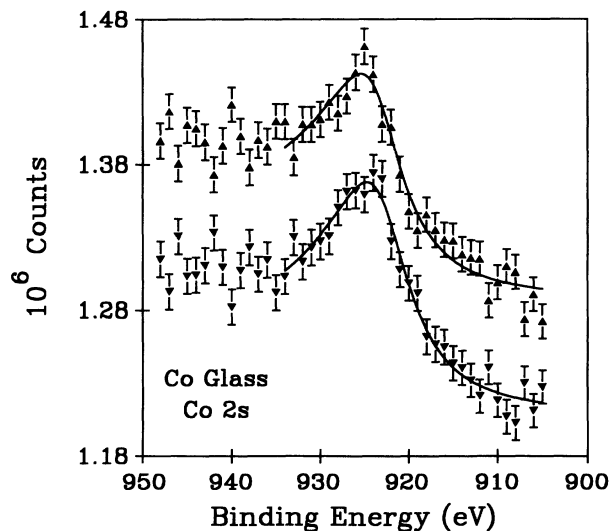


FIG. 11. Separate  $N\uparrow$  and  $N\downarrow$  SRXPS spectra for Co  $2s$  majority-spin ( $\blacktriangle$ ) and minority-spin ( $\blacktriangledown$ ) photoelectrons of  $\text{Co}_{66}\text{Fe}_4\text{Ni}_1\text{B}_{14}\text{Si}_{15}$ . The lines through the data are the result of a simplex fit to each spin component using a single Doniach-Sunjić line shape convoluted with a Gaussian of 1.6-eV FWHM. The binding-energy range for the fit was 934–905 eV.

$I\uparrow/I\downarrow = 1.0 \pm 0.1$ . An "exchange splitting" of  $0.49 \pm 0.3$  eV is observed. As was the case with the Co  $2p_{3/2}$  level, the reduced spin splitting for the glass Co  $2s$  level can be attributed to the reduced valence spin polarization (and therefore a reduced core-valence exchange interaction) of the Co glass relative to the metal. One might suspect that the  $2s$ - $3d$  exchange interaction would be larger than that for the  $2p_{3/2}$  level because the  $2s$  orbital has a  $\sim 25\%$  increased radial extent relative to the  $2p_{3/2}$  level.<sup>43</sup> But this explanation cannot account for the fourfold difference in spin-dependent splittings between the  $2s$  and  $2p_{3/2}$  levels. Note that for the magnetic glass, the  $2s$   $\Gamma\uparrow$  and  $\Gamma\downarrow$  values are similar, and near the average of the  $\Gamma\uparrow$  and  $\Gamma\downarrow$  values for Co metal. Thus the decrease in the valence spin diminishes the spin dependence of the  $L_1L_{2,3}V$  Coster-Kronig transitions. The convergence of the Co  $2s$   $\Gamma\uparrow$  and  $\Gamma\downarrow$  values toward the average value indicates a decrease in the  $\uparrow$ -spin  $3d$  population and an increase in the  $\downarrow$ -spin  $3d$  population (per Co atom), as was inferred from the  $2p_{3/2}$  measurements. Again, this is consistent with spin pairing in the Co valence band upon alloying with B and Si metalloids. The differences observed in Fig. 9 between the Co  $2s$  XPS spectra for the pure metal and glass are therefore due to a larger exchange splitting and a larger  $\Gamma\uparrow$  for the metallic  $2s$  line shape.

#### Co 3p results

High-resolution XPS spectra of the Co  $3p$  level for the glass and the metal are compared in Fig. 12, where again the peaks have been normalized at the peak maxima, and the glass spectrum has been shifted to lower binding energy by 0.3 eV. The  $3p$  spectrum is *a priori* more complicated than the  $2p$  spectra due to the incompletely

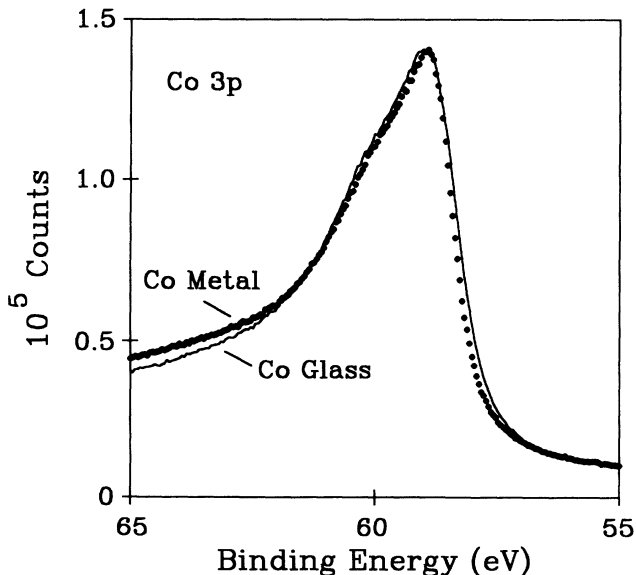


FIG. 12. HRXPS spectra for the Co  $3p$  level of Co metal (dots) and  $\text{Co}_{66}\text{Fe}_4\text{Ni}_1\text{B}_{14}\text{Si}_{15}$  (line). The spectra have been normalized at the peak maxima. The glass spectrum has been shifted 0.3 eV toward lower binding energy to clarify the comparison.

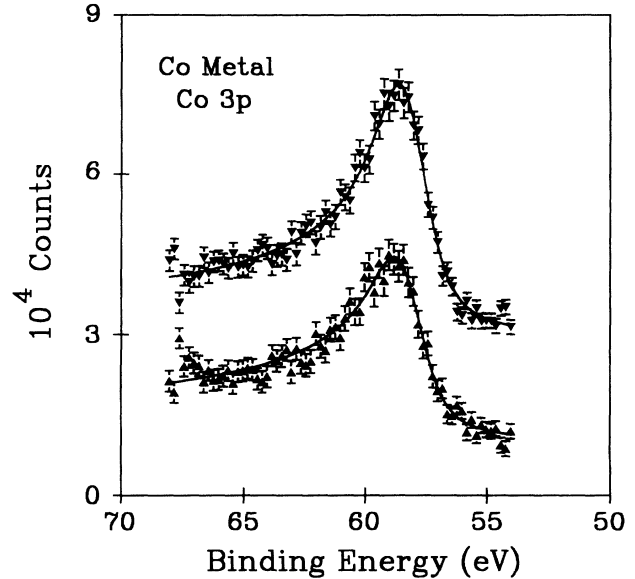


FIG. 13. Separate  $N\uparrow$  and  $N\downarrow$  SRXPS spectra for Co  $3p$  majority-spin ( $\blacktriangle$ ) and minority-spin ( $\blacktriangledown$ ) photoelectrons of Co metal. The lines through the data are the result of a simplex fit to each spin component using a single Doniach-Sunjić line shape convoluted with a Gaussian of 1.6-eV FWHM. The  $N\downarrow$  component has been shifted vertically by 20000 counts for clarity.

resolved spin-orbit components of the  $3p$  level. The comparison in Fig. 12 suggests that the overall  $3p$  line shapes for the metal and glass are quite similar, with the Co-glass  $3p$  spectrum being slightly broader.

Figures 13 and 14 display SRXPS spectra for the Co  $3p$  level for Co metal and glass, respectively. For clarity, the

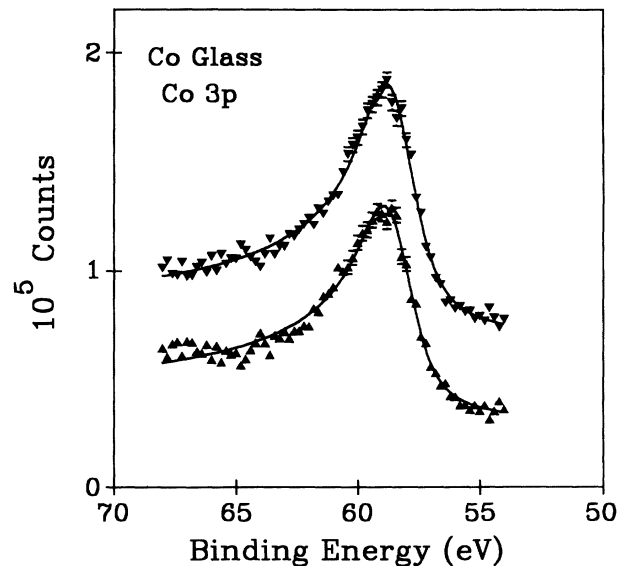


FIG. 14. Separate  $N\uparrow$  and  $N\downarrow$  SRXPS spectra for Co  $3p$  majority-spin ( $\blacktriangle$ ) and minority-spin ( $\blacktriangledown$ ) photoelectrons of  $\text{Co}_{66}\text{Fe}_4\text{Ni}_1\text{B}_{14}\text{Si}_{15}$ . The lines through the data are the result of a simplex fit to each spin component using a single Doniach-Sunjić line shape convoluted with a Gaussian of 1.6-eV FWHM. The  $N\downarrow$  spectrum has been shifted vertically by 40000 counts for clarity.



$N\downarrow$  component has been rigidly shifted vertically by 20 000 and 40 000 counts for Figs. 13 and 14, respectively. Both  $N\uparrow$  and  $N\downarrow$  components are fit well with single DS line shapes. The spectral parameters for  $N\uparrow$  are  $E_B\uparrow = 58.24 \pm 0.03$ ,  $\alpha\uparrow = 0.46 \pm 0.02$ , and  $\Gamma\uparrow = 1.3 \pm 0.1$  eV; and for  $N\downarrow$ ,  $E_B\downarrow = 58.14 \pm 0.03$  eV,  $\alpha\downarrow = 0.38 \pm 0.02$ , and  $\Gamma\downarrow = 1.4 \pm 0.1$  eV. The  $I\uparrow/I\downarrow$  ratio is  $0.81 \pm 0.04$ . A Co-metal  $3p$  exchange splitting of  $0.10 \pm 0.05$  eV is observed. This is smaller than the  $0.3 \pm 0.15$  eV  $3p$  splitting reported for Co metal by Clemens *et al.*<sup>53</sup> It should be noted, however, that the data of Ref. 53 were not fit to line shapes, and the spin splitting was estimated as the difference between peak maxima. As discussed previously, for asymmetric peaks broadened symmetrically by instrumental and lifetime effects, the peak maximum is not a reliable indicator of peak position. For the Co  $3p$  parameters derived in our work, the  $N\uparrow$  peak maximum appears to be shifted an additional 0.07 eV to higher binding energy than the  $N\downarrow$  peak maximum, simply due to the spin dependence of the singularity index  $\alpha$  and the Lorentzian lifetime  $\Gamma$ . The separation of the SRXPS  $3p$  peak maxima for the metal is thus 0.17 eV.

The Co-glass  $3p$  SRXPS data of Fig. 14 also can be fit well by single DS line shapes. For  $N\uparrow$  we derive  $E_B\uparrow = 58.44 \pm 0.03$  eV,  $\alpha\uparrow = 0.41 \pm 0.02$ , and  $\Gamma\uparrow = 1.4 \pm 0.1$  eV. For  $N\downarrow$  we derive  $E_B\downarrow = 58.41 \pm 0.03$  eV,  $\alpha\downarrow = 0.36 \pm 0.02$ , and  $\Gamma\downarrow = 1.6 \pm 0.1$  eV. The glass-Co  $3p$  intensity ratio is  $I\uparrow/I\downarrow = 0.90 \pm 0.03$ . The Co-glass  $3p$  exchange splitting ( $0.03 \pm 0.05$  eV) is essentially undetectable given the error of the measurement. The reduced value of the spin splitting relative to the metal is again consistent with the reduced valence spin polarization of the cobalt glass relative to the metal, in agreement with  $2p_{3/2}$  and  $2s$  results. Note also that the spin-dependent variation in the  $3p$  singularity index  $\alpha$  is somewhat reduced in the glass relative to the metal, in qualitative agreement with  $2p_{1/2}$  results.

It would have been interesting to compare SRXPS spectra for the Co  $3s$  level for metal and glass. Unfortunately, the Si  $2p$  peak interferes with the Co  $3s$  level, rendering accurate measurement of the Co  $3s$  level impossible for the glass. HRXPS and SRXPS spectra for the Co-metal  $3s$  level are discussed in detail elsewhere.<sup>54</sup>

#### IV. RELATIONSHIP TO PRIOR WORK

It is clear from these studies that the core-valence exchange interaction is sizable and observable for deep-core-level photoemission from Co. Therefore, any quantitative description of physical processes involving deep core holes in ferromagnets, such as the  $L_3XX$  Auger transitions, or x-ray absorption from the  $L_{2,3}$  levels, must explicitly include the spin-dependent splittings of these deep levels. For example, it has been shown by Kotani and Mizuta that the theoretical spin polarization of  $L_3M_{2,3}M_{2,3}$  Auger spectra of Fe depends sensitively on the  $2p$ - $3d$  exchange coupling adopted in the theory.<sup>55</sup> SRXPS and HRXPS studies of  $\text{Co}_{66}\text{Fe}_4\text{Ni}_{14}\text{Si}_{15}$  have explicitly shown that as the valence spin polarization decreases, the spin-dependent splittings of the core-level peaks decrease. This finding is supported by recent

SRXPS studies of Fe.<sup>56</sup> The spin-dependent splittings for the Fe  $2p_{3/2}$  ( $0.48 \pm 0.05$  eV), Fe  $2s$  ( $1.2 \pm 0.3$  eV), and Fe  $3p$  ( $0.26 \pm 0.05$ ) levels are all larger than their Co counterparts, due to the larger atomic magnetic moment of ferromagnetic Fe ( $2.22\mu_B$ ).

There is very little theoretical work concerning the nature of the core-valence exchange interaction in itinerant metals. Kakehashi has performed calculations<sup>57</sup> treating the core-valence exchange with varying degrees of valence-band delocalization. However, large simplifications concerning the valence band preclude a meaningful comparison with experiment. In a general sense, our SRXPS results agree with the theory of Kakehashi in that the core-valence exchange interaction leads to a spin splitting of the core-level spectra for which the  $N\uparrow$  component has a larger binding energy than the  $N\downarrow$  component.

The DS line-shape singularity index  $\alpha$  is generally larger for the  $N\uparrow$  Co SRXPS components than for the corresponding  $N\downarrow$  components. This indicates that the  $e$ - $h$  pair excitation spectrum accompanying core-hole creation is intrinsically spin dependent and is stronger for the majority-spin core hole. This phenomenon was also seen in our SRXPS studies of metallic Fe.<sup>56</sup> The *intrinsic* excitation of  $e$ - $h$  pairs by the creation of a spin-dependent core hole is conceptually distinct from the *extrinsic* excitation of  $e$ - $h$  pairs by low-energy electron scattering that produces the secondary electron majority-spin polarization enhancement at low energies in  $3d$  ferromagnets.<sup>39</sup> It may be that photoelectric emission of an  $\uparrow$ -spin core-level electron appears to the valence-band electrons as a sudden net increase in the  $\downarrow$ -spin electron density in the core level. Such an increase in  $\downarrow$ -spin core character could induce a spin-conserving (Coulombic) transition of a  $\downarrow$ -spin valence electron into the unoccupied portion of the  $\downarrow$ -spin  $3d$  valence band. This excitation would have a higher probability than the excitation of an  $\uparrow$ -spin valence electron (caused by  $\downarrow$ -spin core-level emission), because there are virtually no unoccupied  $\uparrow$ -spin states in the Co valence band. This speculative scenario would cause the preferential emission of reduced-energy majority-spin photoelectrons in the asymmetric tail of the  $N\uparrow$  SRXPS peaks, leading to the enhanced values of  $\alpha\uparrow$ . There is virtually no theoretical work concerning the sensitivity of the metallic  $N - 1$  electron response to the spin of a core hole. Previous calculations<sup>24-26</sup> of the itinerant  $e$ - $h$  pair response to core-hole creation treat the core hole as spinless.

The  $2p_{3/2}$  and  $2s$  SRXPS results suggest that core-hole lifetimes (as determined by Auger rates) are generally spin dependent, and that the  $L_1L_{2,3}V$  Coster-Kronig transition rate is particularly sensitive to the spin of the  $2s$  hole. The data are consistent with spin conservation in both Auger transitions and Coster-Kronig transitions involving the valence band, with the excess of  $\uparrow$ -spin electrons in the valence band producing the observed spin dependence. Similar results were found for Fe.<sup>56</sup> There is virtually no previous theoretical work concerning these dependencies. It is our hope that the SRXPS results presented here and elsewhere<sup>54,56</sup> stimulate theoretical interest in the rich spin dependence of core-level photo-

emission from ferromagnetic metals.

We believe that SRXPS measurements will provide a great deal of information concerning interface and thin-film magnetism. SRXPS measurements of the  $2p_{3/2}$  level of  $3d$  transition metals should be particularly useful. Such measurements are highly element specific due to the large energy difference between the  $2p_{3/2}$  binding energies in the  $3d$  transition series. The  $2p_{3/2}$  peaks are the most intense in the XPS spectrum. Such SRXPS studies should not suffer from vagaries introduced by spin-dependent elastic scattering during transport of the photoelectrons out of the solid.<sup>58</sup> The kinetic energies of the SRXPS spectra usually exceed 300 eV where, from a theoretical point of view,<sup>59</sup> spin-dependent scattering should be negligible. Thus the SRXPS data reflect the intrinsic spin dependence of the photoelectric excitation. The data presented here clearly indicate the sensitivity of the SRXPS spectra to a variation in the atomic magnetic moment. The extent to which quantitative information regarding the atomic magnetic moment can be extracted from a given SRXPS spectrum will depend on future experimental and theoretical progress.

## V. CONCLUSIONS

The role of electron spin in photoelectric emission from the  $2s$ ,  $2p_{1/2}$ ,  $2p_{3/2}$ , and  $3p$  core levels of cobalt metal was investigated through a combination of spin-resolved x-ray-photoelectron spectroscopy (SRXPS) and high-energy-resolution x-ray-photoelectron spectroscopy (HRXPS) studies. The sensitivity of the Co core-level

spectra to a variation in the valence spin polarization was revealed by comparing the Co-metal data with SRXPS and HRXPS spectra from the amorphous cobalt-based ferromagnetic glass  $\text{Co}_{66}\text{Fe}_4\text{Ni}_1\text{B}_{14}\text{Si}_{15}$ . The results demonstrate the role of intra-atomic exchange in deep-core-level photoemission from Co, and reveal core-hole spin dependencies for core-hole-induced electron-hole pair excitation, for the  $L_1L_{2,3}V$  Coster-Kronig transition probability, and for the transition rates of Auger transitions involving the valence band. The data also suggest that the reduction of the cobalt magnetic moment in the  $\text{Co}_{66}\text{Fe}_4\text{Ni}_1\text{B}_{14}\text{Si}_{15}$  glass results from the transfer of majority-spin  $3d$  electron density into the minority-spin  $3d$  band, caused by a hybridization-induced weakening of the  $3d$  electron-electron interaction.

## ACKNOWLEDGMENTS

This paper is based upon work supported by the National Science Foundation under Grant No. CHE-9117138. Acknowledgment is made to the donors of the Petroleum Research Fund, administered by the American Chemical Society, for partial support of the research. Financial support also came from the Camille and Henry Dreyfus Foundation, The Charles A. Dana Foundation, and Lehigh University. R.J.P. acknowledges support from the U.S.D.E. The authors acknowledge the allocation of time and services in the SCIENTA ESCA Laboratory of Lehigh University. The technical assistance of Dr. Alfred C. Miller is appreciated.

\*Author to whom correspondence should be addressed.

<sup>1</sup>C. S. Fadley, D. A. Shirley, A. J. Freeman, P. S. Bagus, and J. V. Mallow, *Phys. Rev. Lett.* **23**, 1397 (1969).

<sup>2</sup>J. C. Carver, G. K. Schweitzer, and T. A. Carlson, *J. Chem. Phys.* **57**, 973 (1972).

<sup>3</sup>S. Hufner and G. K. Wertheim, *Phys. Rev. B* **7**, 2333 (1973).

<sup>4</sup>G. K. Wertheim, S. Hufner, and H. J. Guggenheim, *Phys. Rev. B* **7**, 556 (1973).

<sup>5</sup>S. P. Kowalczyk, L. Ley, R. A. Pollak, F. R. McFeely, and D. A. Shirley, *Phys. Rev. B* **7**, 4009 (1973).

<sup>6</sup>S. L. Qiu, R. G. Jordan, A. M. Begley, X. Wang, Y. Liu, and M. W. Ruckman, *Phys. Rev. B* **46**, 13 004 (1992).

<sup>7</sup>J. F. Van Acker, Z. M. Stadnik, J. C. Fuggle, H. J. W. M. Hoekstra, K. H. J. Bushow, and G. Stroink, *Phys. Rev. B* **37**, 6827 (1988).

<sup>8</sup>F. U. Hillebrecht, R. Jungblut, and E. Kisker, *Phys. Rev. Lett.* **65**, 2450 (1990).

<sup>9</sup>C. Carbone, T. Kachel, R. Rochow, and W. Gudat, *Solid State Commun.* **77**, 619 (1991).

<sup>10</sup>V. Kinsinger, I. Sander, P. Steiner, R. Zimmermann, and S. Hufner, *Solid State Commun.* **73**, 527 (1990).

<sup>11</sup>L. E. Klebanoff and D. A. Shirley, *Phys. Rev. B* **33**, 5301 (1986).

<sup>12</sup>B. Hermsmeier, C. S. Fadley, M. O. Krause, J. Jimenez-Mier, P. Gerard, and S. T. Manson, *Phys. Rev. Lett.* **61**, 2592 (1988).

<sup>13</sup>S. P. Kowalczyk, Ph.D. Thesis, University of California, Berkeley, 1976.

<sup>14</sup>F. R. McFeely, S. P. Kowalczyk, L. Ley, and D. A. Shirley, *Solid State Commun.* **15**, 1051 (1974).

<sup>15</sup>S. J. Oh, G. H. Gweon, and J. G. Park, *Phys. Rev. Lett.* **68**, 2850 (1992).

<sup>16</sup>B. W. Veal and A. P. Paulikas, *Phys. Rev. Lett.* **51**, 1995 (1983).

<sup>17</sup>J. R. Leite, J. C. Rodrigues, A. C. Ferraz, and A. C. Pavao, *Phys. Rev. B* **16**, 978 (1977).

<sup>18</sup>P. S. Bagus, A. J. Freeman, and F. Sasaki, *Phys. Rev. Lett.* **30**, 850 (1973).

<sup>19</sup>R. P. Gupta and S. K. Sen, *Phys. Rev. B* **10**, 71 (1974).

<sup>20</sup>K. Okada and A. Kotani, *J. Phys. Soc. Jpn.* **61**, 4619 (1992).

<sup>21</sup>K. Okada, A. Kotani, and B. T. Thole, *J. Electron. Spectrosc. Relat. Phenom.* **58**, 325 (1992).

<sup>22</sup>B. T. Thole and G. van der Laan, *Phys. Rev. B* **44**, 12 424 (1991).

<sup>23</sup>D. A. Shirley, in *Topics in Applied Physics, Photoemission in Solids I*, edited by M. Cardona and L. Ley (Springer-Verlag, Berlin, 1978), p. 165.

<sup>24</sup>P. Nozieres and C. T. DeDominicis, *Phys. Rev.* **178**, 1084 (1969).

<sup>25</sup>G. D. Mahan, *Phys. Rev. B* **11**, 4814 (1975).

<sup>26</sup>S. Doniach and M. Sunjic, *J. Phys. C* **3**, 285 (1970).

<sup>27</sup>L. A. Feldkamp and L. C. Davis, *Phys. Rev. B* **22**, 3644 (1980).

<sup>28</sup>D. R. Penn, *Phys. Rev. Lett.* **42**, 921 (1979).

<sup>29</sup>R. H. Victora and L. M. Falicov, *Phys. Rev. Lett.* **55**, 1140 (1985).

- <sup>30</sup>C. Kittel, *Solid State Physics* (Wiley, New York, 1976), p. 465.
- <sup>31</sup>D. Raskin and C. H. Smith, in *Amorphous Metallic Alloys*, edited by F. E. Luborsky (Buttersworth, London, 1980), p. 381.
- <sup>32</sup>Metglas Alloy 2714A from Allied Signal, Inc.
- <sup>33</sup>A HRXPS analysis of the cobalt glass gave B/Co and Si/Co atomic ratios of  $0.28 \pm 0.04$  and  $0.22 \pm 0.04$ , respectively. The theoretical values based on the formula  $\text{Co}_{66}\text{Fe}_4\text{Ni}_{14}\text{Si}_{15}$  are 0.22 and 0.23, respectively. The Fe and Ni content of the glass could not be quantitatively evaluated.
- <sup>34</sup>L. E. Klebanoff, D. G. Van Campen, and R. J. Pouliot, *Rev. Sci. Instrum.* **64**, 2863 (1993).
- <sup>35</sup>M. R. Scheinfein, D. T. Pierce, J. Unguris, J. J. McClelland, R. J. Celotta, and M. H. Kelly, *Rev. Sci. Instrum.* **60**, 1 (1989).
- <sup>36</sup>J. Kessler, *Polarized Electrons* (Springer-Verlag, Berlin, 1985), pp. 234 and 243.
- <sup>37</sup>Sherman function values measured during the SRXPS data acquisition and used in the spectral analysis were as follows: Co metal,  $S = 0.080$  ( $2p_{3/2}$ ,  $2p_{1/2}$ ), 0.055 ( $3p$ ), and 0.035 ( $2s$ ); Co glass,  $S = 0.075$  ( $2p_{3/2}$ ), 0.074 ( $2p_{1/2}$ ), 0.073 ( $3p$ ), and 0.068 ( $2s$ ). The Co metal  $2s$  and  $3p$  data were collected prior to full spin detector optimization (Ref. 34). The systematic error in the Sherman function is 10% of the value ( $0.080 \pm 0.008$ ). See Ref. 34 for details of the spin detector calibration.
- <sup>38</sup>H. Hopster, *Phys. Rev. B* **36**, 2325 (1987).
- <sup>39</sup>E. Kisker, W. Gudat, and K. Schroder, *Solid State Commun.* **44**, 591 (1982).
- <sup>40</sup>R. Alben, J. I. Budnick, and G. S. Cargill III, in *Metallic Glasses*, edited by J. J. Gilman and H. J. Leamy (American Society for Metals, Metals Park, 1978), p. 310.
- <sup>41</sup>R. Hasegawa and R. Ray, *J. Appl. Phys.* **50**, 1586 (1979).
- <sup>42</sup>For a discussion, see R. C. O'Handley, in *Amorphous Metallic Alloys*, edited by F. E. Luborsky (Buttersworth, London, 1983), p. 381.
- <sup>43</sup>R. D. Cowan, *Theory of Atomic Structure and Spectra* (University of California Press, Berkeley, 1981), p. 236.
- <sup>44</sup>See E. H. S. Burhop, *The Auger Effect and Other Radiationless Transitions* (Cambridge University Press, Cambridge, 1952), p. 11.
- <sup>45</sup>This mechanism has been put forward for in spin-resolved Fe  $3p$  photoemission studies: C. Carbone and E. Kisker, *Solid State Commun.* **65**, 1107 (1988).
- <sup>46</sup>K. Yamauchi and T. Mizoguchi, *J. Phys. Soc. Jpn.* **39**, 541 (1975).
- <sup>47</sup>P. H. Citrin, G. K. Wertheim, and Y. Baer, *Phys. Rev. B* **16**, 4256 (1977).
- <sup>48</sup>The extrinsic loss contribution to the XPS line shape can be assessed by scattering externally generated electrons from the sample with the same kinetic energy as the XPS peak in question, and measuring the energy-loss spectrum. The extrinsic loss intensity within  $\sim 10$  eV from the zero loss peak is only  $\sim 2-3\%$  of the elastic peak intensity. This extrinsic intensity is not significant in comparison to the asymmetric intensity observed in the SRXPS and HRXPS spectra.
- <sup>49</sup>G. van der Laan and B. T. Thole, *Phys. Rev. B* **42**, 6670 (1990).
- <sup>50</sup>S. Raaen, *Solid State Commun.* **60**, 991 (1986).
- <sup>51</sup>Fits over the entire  $2s$  data range of 945–905 eV agreed poorly with the high-binding-energy region of the  $N\downarrow 2s$  spectrum.
- <sup>52</sup>E. J. McGuire, *Phys. Rev. A* **3**, 587 (1971).
- <sup>53</sup>W. Clemens, E. Vescovo, T. Kachel, C. Carbone, and W. Eberhardt, *Phys. Rev. B* **46**, 4198 (1992).
- <sup>54</sup>D. G. Van Campen and L. E. Klebanoff, preceding paper *Phys. Rev. B* **49**, 2040 (1994).
- <sup>55</sup>A. Kotani and H. Mizuta, *Solid State Commun.* **51**, 727 (1984).
- <sup>56</sup>D. G. Van Campen, R. J. Pouliot, and L. E. Klebanoff, *Phys. Rev. B* **48**, 17533 (1993).
- <sup>57</sup>Y. Kakehashi, *Phys. Rev. B* **32**, 1607 (1985), and references therein.
- <sup>58</sup>D. P. Pappas, K.-P. Kamper, B. P. Miller, H. Hopster, D. E. Fowler, C. R. Brundle, A. C. Luntz, and Z.-X. Shen, *Phys. Rev. Lett.* **66**, 504 (1991).
- <sup>59</sup>J. A. D. Matthew, *Phys. Rev. B* **25**, 3326 (1982).